Journal of
Materials Chemistry B

Accepted Manuscript

This is an *Accepted Manuscript*, which has been through the RSC Publishing peer review process and has been accepted for publication.

Accepted Manuscripts are published online shortly after acceptance, which is prior to technical editing, formatting and proof reading. This free service from RSC Publishing allows authors to make their results available to the community, in citable form, before publication of the edited article. This *Accepted Manuscript* will be replaced by the edited and formatted *Advance Article* as soon as this is available.

To cite this manuscript please use its permanent Digital Object Identifier (DOI®), which is identical for all formats of publication.

More information about *Accepted Manuscripts* can be found in the **Information for Authors**.

Please note that technical editing may introduce minor changes to the text and/or graphics contained in the manuscript submitted by the author(s) which may alter content, and that the standard **Terms & Conditions** and the **ethical guidelines** that apply to the journal are still applicable. In no event shall the RSC be held responsible for any errors or omissions in these *Accepted Manuscript* manuscripts or any consequences arising from the use of any information contained in them.

Journal of Materials Chemistry-B

Dynamic Article Links ►

Cite this: DOI: 10.1039/c0xx00000x

Full ARTICLE

www.rsc.org/xxxxxx

Glucomannan-poly(N-vinyl pyrrolidinone) bicomponent hydrogels for wound healing

Munira Shahbuddin,[ab] Anthony J. Bullock,[a] Sheila MacNeil,[a] and Stephen Rimmer [b*]

Received (in XXX, XXX) Xth XXXXXXXXX 20XX, Accepted Xth XXXXXXXXX 20XX

DOI: 10.1039/b000000x

Polysaccharides interact with cells in ways that can be conducive to wound healing. We have recently reported that Konjac glucomannan (KGM) which is comprised of D-mannose and D-glucose linked by β1-4 glycosidic chains, stimulates fibroblast proliferation. The aim of this study was to produce a range of crosslinked KGMs and bicomponent KGM containing hydrogels and to examine their potential for wound healing. Two types of KGM hydrogel were synthesized, biodegradable from crosslinked KGM and non-biodegradable by forming semi-IPN and graft-conetworks with a second synthetic component, poly(N-vinyl pyrrolidinone-co-poly(ethylene glycol)diacrylate) (P(NVP-co-PEGDA)), which was produced by UV initiated radical polymerization. Crosslinked KGM was formed by bimolecular termination of macro-radicals formed by oxidation with Ce(IV). Semi-IPNs were formed by copolymerization of NVP and PEGDA in the presence of KGM and in the graft-conetworks the KGM was also crosslinked using the Ce(IV) procedure. The hydrogels had different swelling properties and differences could be observed in their chemical structure using ^{13}C solid state NMR, DSC and FTIR. Both forms were cytocompatible but only the graft-conetworks had the ability to stimulate fibroblast metabolic activity and to stimulate the migration of both fibroblasts and keratinocytes. In conclusion a form of KGM hydrogel has been produced that could benefit wound healing.

1. Introduction

Konjac glucomannan (KGM) is a linear, neutral polysaccharide derived from the tuber of *Amorphophallus konjac C. Koch*. Structurally it consists of D-glucose and D-mannose linked by β-1,4 linkage in a molar ratio of 1.6:1 with an acetyl group attached to 1 out of every 19 sugar residues [1]. It has been reported to be biocompatible, capable of supporting cells in culture and delivering drugs [2-4], and we have recently shown that it stimulates fibroblast proliferation while paradoxically it inhibits keratinocyte proliferation [5]. The aim of this study is to develop hydrogels containing KGM that might be useful for stimulating wound healing. Non-modified KGM forms a hydrogel rapidly, swelling up to 20 fold, but it degrades quickly in moist environments [6]. Ideally it would be useful to control KGM's swelling to create a highly hydrated hydrogel which could be easily handled for application to wounds [7, 8].

In recent years, hydrogels based on heteropolysaccharides have received considerable attention [9-11]. Hydrogels for wound dressings are attractive because of their hydrophilicity, and flexibility and properties can be altered by the degree of crosslinking of the hydrogel [12-14]. Several studies have proposed that hydrogel wound dressings can enhance wound healing but the evidence reported is only partially convincing[15]. The mechanical and physical properties of KGM hydrogels have been improved by crosslinking with other synthetic or natural polymers, or by chemical modification using methylation, enzymatic hydrolysis or UV irradiation [9, 16, 17].

In this study, three forms of hydrogel were made and examined. The first of these was a biodegradable hydrogel made by crosslinking KGM using cerium ammonium nitrate (Ce(IV)). The two other classes were bicomponent hydrogels with either semi interpenetrating network (semi-IPN) or graft-conetwork architectures. The semi-IPNs were made by copolymerizing poly(N-vinyl pyrrolidinone (PNVP) and Poly(ethylene glycol diacrylate) (PEGDA) with KGM using 2-hydroxy-2-methylpropiophenone (HMPP) as an initiator with UV curing. Graft-networks were also produced by UV-initiated polymerization of NVP and PEGDA but prior to this step the KGM was crosslinked and grafted with NVP/PEGDA using Ce(IV). A blend of two or more polymers by physical entanglement where each individual network may be formed simultaneously or sequentially is called an interpenetrating network (IPN) [18, 19]. Semi-IPNs are formed when only one polymer in the system is crosslinked, while a graft-conetwork is formed when crosslinking occurs between two or more interpenetrating polymer networks [20]. As already mentioned our aim was to use the stimulatory properties in a format that could be easily handled. KGM hydrogels do not have sufficient mechanical strength to provide good handling properties.

Therefore, to achieve the required physical properties we added a second hydrogel component with permanent crosslinks: poly(N-vinyl prolidinone-co-poly(ethylene glycol diacrylate)) (P(NVP-*co*-PEGDA).

In this study, PNVP was chosen as it is a water soluble homopolymer commonly used in wound dressings and biomedical applications [21]. PNVP can be conjugated to a number of drugs and polymers for pharmaceutical applications [22], and previous work from this laboratory demonstrated the cytocompatibility of PNVP copolymerized with ethandiol dimethacrylate or diethylene glycol bisallylcarbonate in both direct and indirect contact with human dermal fibroblasts [23]. This study also showed that while fibroblasts did not attach to this hydrogel, the presence of PNVP adjacent to the cells significantly increased fibroblast viability [23].

In the current study the crosslinked KGM and bicomponent hydrogels were characterized by DSC, ^{13}C NMR, and FTIR. Following our previous observations of the stimulation of fibroblast cells by both KGM and PNVP-based hydrogels[22] it seemed reasonable to combine the two systems and to use the physical properties of crosslinked PNVP hydrogels to enhance the handling characteristics of KGM-based materials. The ability of several KGM-NVP bicomponent hydrogels to stimulate fibroblast and keratinocyte metabolic activity and migration was determined in an initial study aimed at developing wound dressings that could assist the healing processes.

2. Experimental Section

2.1 Materials

The monomer N-vinyl-2-pyrrolidinone (NVP, ≥99%, Aldrich) was purified by distillation at reduced pressure and stored at 4°C until use. Konjac glucomannan (KGM 97%, Health Plus Ltd, U.K.) was used as supplied. Poly(ethylene glycol) diacrylate (PEGDA) and the initiators, 2-hydroxy-2-methylpropiophenone (HMPP, 97%) and cerium ammonium nitrate (Ce(IV)), sodium chloride (NaCl), hydrochloric acid (HCl), 3-(4,5-dimethylthiazol-2-yl)-2-5-diphenyltetrazolium bromide (MTT), isopropanol and Cellusolve (2-ethoxy ethanol) were supplied by Sigma Aldrich, Poole, U.K.. 3.7% of formaldehyde, SYTO9 (Molecular Probes, U.S.), Propidium Iodide (PI) (Invitrogen, U.K.) and plasticwares for cell culture (Costar, U.K.).

2.2 Synthesis and preparation of crosslinked KGM hydrogels using Ce(IV) ammonium nitrate

Crosslinked KGM hydrogels were prepared by bimolecular coupling of macro-radicals generated by action of Ce(IV). Two sets of hydrogels were made by either varying concentrations of KGM (0.5, 1.0, 1.25 and 1.5%) with $1x10^{-3}$ % Ce(IV) remaining constant, or varying concentration of Ce(IV) ($1x10^{-3}$, $1.5x10^{-3}$, $3x10^{-3}$ and $6x10^{-3}$%) with 1.0 % KGM remaining constant. KGM was dissolved in 160 mL dH_2O with vigorous stirring for 30 minutes at room temperature to form a uniform solution. Degassing with nitrogen gas was conducted prior to reaction with Ce(IV), to remove oxygen and to improve mixing. Ce(IV) was then added to the solution and mixed thoroughly. The solution was poured into a Petri dish (140x20 mm), covered with PTFE film, and left to evaporate at room temperature for 2 - 4 days.

2.3 Synthesis and preparation of semi-IPNs and graft-conetworks of KGM (P(NVP-co-PEGDA) hydrogels

Semi-IPNs were prepared by free radical polymerization using 2% 2-hydroxy-2-methylpropiophenone (HMPP) as initiator. 25 mL dH_2O was added to 10 g of NVP and mixed thoroughly for 30 minutes. Then KGM (14, 24, and 35% w/v) was added to the solution and stirred well for 30 minutes. 2 g of PEGDA with 2% HMPP was then added to the solution and stirred well for 30 minutes. Using a syringe, the solution was then injected into a pre-made mould of dimensions 7.5cm x7.5cm x 0.25cm, consisting of two PTFE film covered quartz plates. The mould was UV irradiated for a total of 6 minutes, (3 minutes on each side). The resulting hydrogel was removed from the mould, placed in 70% ethanol and rocked gently for 3 days to remove unreacted monomers. The ethanol was changed daily before washing twice in PBS. The hydrogels were then stored in PBS. For graft-conetworks, the hydrogels were prepared as per the semi-IPNs but 0.5 or 1% Ce(IV) was added and the mixture was stirred for 1 hour prior to placing in the mould for UV polymerization.

2.4 Cell culture

Human fibroblasts and keratinocytes were isolated from skin removed during abdominoplasty or breast reduction elective surgeries in the Department of Plastic Surgery, Northern General Hospital, Sheffield with fully informed patient consent for the use of skin for experimental research. Fibroblasts were isolated from skin by mincing the dermal region of the skin into small pieces, followed by digestion with 0.05% collagenase A in DMEM overnight at 37°C with 5% CO_2. The cell suspension was then centrifuged at 400g and resuspended in medium (DMEM supplemented with 10% fetal calf serum (FCS), 0.25 $mg.mL^{-1}$ glutamine, 0.625 $\mu g.mL^{-1}$ amphotericin B, 100 $I.U.mL^{-1}$ penicillin and 100 $\mu g.mL^{-1}$ streptomycin). These cells were then cultured in fibroblast medium in T25 flasks and incubated at 37°C with 5% CO_2. Medium was changed every 2 days and cells were passaged as needed, fibroblasts between passage 4 and 9 were used in experiments. Keratinocytes were extracted from the 0.25 cm^2 skin after an incubation with 10 ml of 1 $mg.mL^{-1}$ Difco Trypsin in PBS overnight at 4°C, trypsin was neutralized by addition of 5 mL FCS followed by the separation of epidermis from the dermis. The underside of the epidermis and the top of the dermis were gently scraped into 10% Green's medium (consisting of DMEM high glucose and Ham's F12 medium in a 3:1 ratio supplemented with 10% FCS, 10 $ng.mL^{-1}$ recombinant human epidermal growth factor, 0.4 $\mu g.mL^{-1}$ hydrocortisone, 0.1 nM cholera toxin, 1.8×10^{-4} M adenine, 5 $mg.mL^{-1}$ insulin, 5 $\mu g.mL^{-1}$ apo-transferrin, $2x10^{-7}$ M 3,3,5-tri-idothyronine, $2x10^{-3}$ M glutamine, 0.625 $\mu g.mL^{-1}$ amphotericin B, 100 $I.U.mL^{-1}$ penicillin and 100 $I.U.mL^{-1}$ streptomycin) to retrieve keratinocytes. The cell suspension was transferred into a 25 mL universal and centrifuged at 180g for 5 minutes. The resulting pellet was resuspended in Green's medium and transferred to a T75 flask that was previously seeded with $5x10^6$ i3T3 to act as a feeder layer. 3T3 fibroblasts were growth arrested by gamma irradiation with a dosage of 60Gy using a ^{137}Cs source to create i3T3 cells. Cells were incubated at 37°C, in a 5% CO_2 in a humidified atmosphere. The medium was changed every 2-3

days, and keratinocytes were passaged at 70-80% confluency. Only keratinocytes at passages 1-2 were used for experiments.

2.5 Measurement of cell proliferation using MTT assay

3-(4,5-dimethylthiazol-2-yl)-2-5-diphenyltetrazolium bromide (MTT) assay was used to measure proliferation of fibroblasts and keratinocytes in tissue culture plastic in direct and indirect contact with KGM containing hydrogels [24]. After removing the hydrogels from each well plate, the cells were washed with PBS and then 1 mL of 0.5 mg.mL^{-1} MTT in PBS was added, and incubated for 1 hour at 37^{o}C. The blue formazan product was eluted using 200 µL of acidified isopropanol (0.1% 1 M HCl). 100 µL eluted formazan were transferred into 96 well plate and the optical density (at 540 nm and referenced at 630 nm) was read in a Dynex Technologies MRXII microplate reader.

2.6 Indirect contact of KGM hydrogels with human primary fibroblasts

1 mL of 2x10^4 fibroblasts in 10% DMEM or 1 mL of 2x10^4 keratinocytes co-cultured with 2x10^4 i3T3 were cultured for 24 hours in 12 well plates respectively and left to attach overnight. 0.79 cm^2 hydrogel was placed in a Thin Cert (0.4 µm) (Greiner Bio-One, Belgium) with 500 µl fresh medium and an additional 500 µL fresh medium was added into the well. Cell proliferation was measured after 3 days of incubation at 37^{o}C, 5% CO_2 using MTT assays.

2.7 Direct contact of KGM hydrogels with human primary fibroblasts and keratinocytes

1 mL of 2x10^4 fibroblasts in 10% DMEM or 1 mL of 2x10^4 keratinocytes co-cultured with 2x10^4 i3T3 were cultured for 24 hours in 12 well plates respectively and left to attach overnight. Then 0.79 cm^2 samples of hydrogel were placed in direct contact with the cells and cell proliferation was measured after 1, 3 and 5 days using MTT assays.

2.8 Live/Dead staining of human primary fibroblasts

1 mL of 2x10^4 fibroblasts were cultured for 24 hours in 12 well plates. Then 0.79cm^2 samples of KGM hydrogels was added in direct contact with the cells. After 3 days, the medium and the hydrogels were removed and the cells were washed with PBS twice. 1 mL of SYTO9 (1 µg.mL^{-1}) and PI (1 µg.mL^{-1}) were added to each sample and incubated at 37°C for 1 hour. The two-colour fluorescence assay was observed using an Axon ImageXpress fluorescence microscope (Axoncorp, USA). The excitation and emission wavelengths for PI and SYTO9 were λ_{ex} 480 nm/λ_{em} 500 nm and λ_{ex} 545 nm/λ_{em} 610 nm respectively.

2.9 Differential Scanning Calorimetry (DSC)

Calorimetric analyses were performed on a Perkin Elmer DSC Pyris-1 (Massachusetts, U.S.A). Each hydrogel was subjected to two heating and cooling cycles between -60 to 60^{o}C at a heating rate of 1^{o} C per minute in a nitrogen atmosphere.

2.10 Equilibrium Water Content (EWC)

The equilibrium water content of the hydrogels by weight was analysed by cutting a circular disc from a sheet of hydrogel swollen in water and then evaporating the water to create dry xerogels. The excess water was removed gently with a paper towel and the swollen weight of the polymer was recorded. The hydrogel was then dried for 24 hours at 50^{o}C in a vacuum oven. The weight of the polymer disc was then recorded every two hours until the weight remained constant. The EWC is defined here as:

$$\text{EWC (\%)} = \frac{W_w - W_d}{W_w} \text{ x } 100$$

Where W_w = wet weight and W_d = dry weight

2.11 Differential scanning calorimetry of hydrated KGM hydrogel

Differential scanning calorimetric analyses were performed using a Perkin Elmer DSC Pyris-1 (Massachusetts, U.S.A) on hydrated KGM hydrogels, soaked in dH_2O overnight prior to analyses. The samples were heated at a rate of 1^{o}C per minute from -60 to 60^{o}C in a nitrogen atmosphere.

2.12 Migration of fibroblasts and keratinocytes in a wound scratch assay

Cell migration was measured by a scratch wound healing assay. 1x10^5 fibroblasts or 1x10^5 keratinocytes co-cultured with 5x10^4 i3T3 each in 1 mL of medium were cultured in 12 well plates until confluent (usually 48 hrs) then a scratch wound was introduced using a 1000 µL tip, which gave a scratch width of 1 mm. The cultures were then washed three times with PBS to remove cell debris, and they were then treated with 300 mL of 10 µg.mL^{-1} mitomycin C in PBS for 30 minutes (for fibroblasts) or 60 minutes (keratinocytes) to growth arrested cells. The medium was then removed and the cultures washed with PBS. 1 mL of fresh medium was added into the culture and the cultures were incubated at 37^{o}C with 5% CO_2 for 48 hours. Cell migration was captured at time intervals of 0, 15, 24, 36 and 48 hours using an Olympus microscope and digital camera at x20 magnification. The area of cell migration into wound site was quantified using ImageJ and presented as relative migration compared with the 0 hour measurement.

2.13 ^{13}C Solid State NMR

^{13}C solid state NMR spectra were obtained at the EPSRC UK National Solid-state NMR Service at Durham using Varian VNMRS 400 with reference to neat tetramethylsilane. The measurement on cross-polarisation was carried out at 1.00ms contact time, 53.2 kHz TPPM decoupling, 6800 Hz spinning rate, 0.010s Gaussian broadening with FT size 16384 in ambient temperature.

2.14 Statistical Analysis

Quantitative data (e.g. MTT optical density readings) were analyzed using Minitab (MiniTab Inc. USA) and Microsoft Excel (Microsoft Corporation) to obtain means and standard deviation (SD), n = number of independent experiments each with three replicates. Student's t-test was performed to determine statistical significance, indicated in the corresponding figures or tables by: ns (not significant; $p \geq 0.05$), * (significant; $p < 0.05$), ** (highly significant; $p < 0.01$) and *** (extremely significant; $p < 0.001$).

3. Results

3.1 Synthesis and Characterization of KGM hydrogels using ^{13}C Solid State NMR, Fourier Transform Infra red (FTIR) and Differential Scanning Calorimetry (DSC).

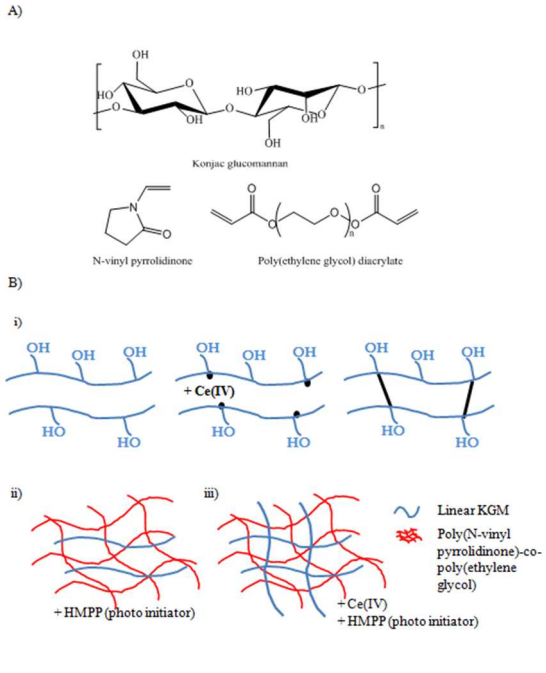

Figure 1. Chemical structures of konjac glucomannan, N-vinyl pyrrolidinone (NVP) and poly(ethylene glycol) diacrylate (PEGDA) B) Schematic representation of the formation of i) crosslinking with linear KGM initiated by Ce(IV), ii) semi-IPN of P(NVP-co-PEGDA) initiated by HMPP with uncrosslinked KGM and iii) grafted conetwork of KGM and P(NVP-co-PEGDA) initiated by Ce(IV) and HMPP

Crosslinked KGM and bicomponent hydrogels were produced in aqueous solution at room temperature using KGM and Ce(IV) at a range of concentrations. Figure 1 depicts the structures of the hydrogels and a scheme of their production. Degradable hydrogels were synthesized using Ce(IV) to cross-link KGM at various concentrations while the non-degradable hydrogels were prepared using photopolymerization to combine KGM with NVP and PEGDA to obtain both semi-IPN and graft-conetwork using 2-hydroxy-2-methylpropiophenone (HMPP) as the photoinitiator.

FTIR spectra, shown in figure 2, of all the crosslinked KGM hydrogels showed the presence of β-1,4 linked glucosidic and β-1,4 linked mannosidic linkages at 1027-1244 cm^{-1} and peaks at 808-875 cm^{-1} which were assigned to mannose and glucose (Figure 2) [25, 26]. These hydrogels exhibited the broad band of the OH groups at about 3300 cm^{-1} [9, 17, 27], accompanied by the peak at 2920 cm^{-1} which is the characteristic stretching of C-H group attached to the hydroxyl group [9, 25]. The characteristic absorption peaks for C6-OH and the bridge C-O-C stretch at 1062 and 1027 cm^{-1} respectively were also observed in all of the KGM containing hydrogels. There were no differences in the spectra of the crosslinked KGM hydrogels with increasing concentration of Ce(IV) (Figure 2B). Figure 2B shows examples of spectra derived from the two biocomponent hydrogels and these are compared to the spectra of single component materials: a crosslinked KGM and P(NVP-co-PEGDA). The peaks at 1493, 1460, 1421, 2013, and 2160 cm^{-1} assigned to CH were observed in the P(NVP-co-PEGDA), semi-IPNs and graft-conetworks but not in the crosslinked KGM. The peaks were more obvious in the graft-conetwork compared to the semi-IPNs.

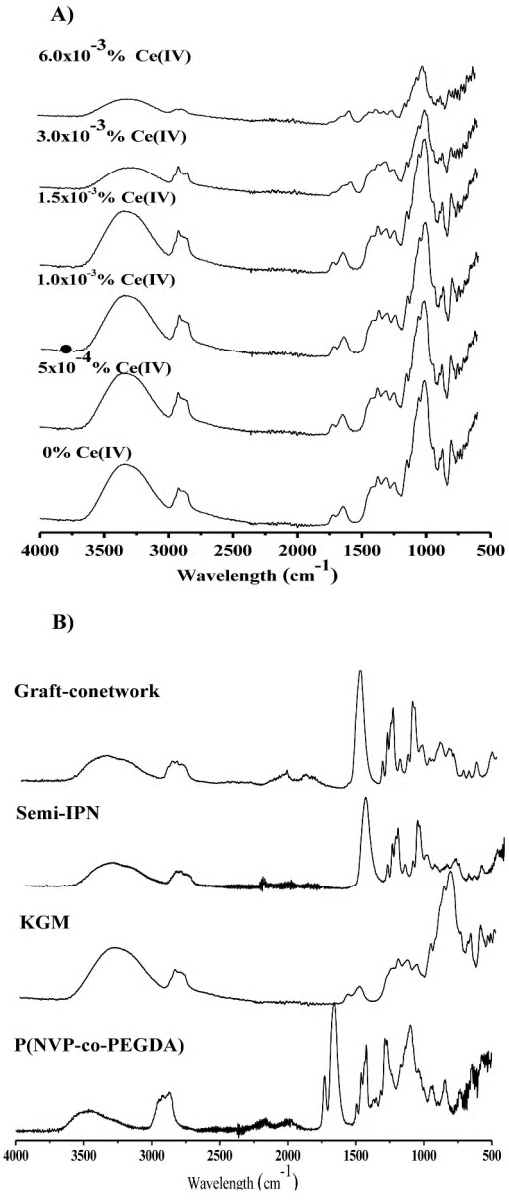

Figure 2. FTIR spectra: A) crosslinked KGM hydrogels with increasing concentrations of Ce(IV); B) graft-conetwork, semi-IPN, crosslinked KGM and P(NVP-co-PEGDA).

In the semi-IPNs and the graft-conetworks the peaks at 1727 to 1648 cm^{-2} were assigned to C=O acetyl group and 1030 to 1095 cm^{-1} was assigned to the C-O and C-N groups respectively[28, 29]. There was a reduction in the intensity of the peaks at 1727 cm^{-1} for C=O and 1635 cm^{-1} for C-O in KGM containing hydrogels, compared to P(NVP-co-PEGDA).

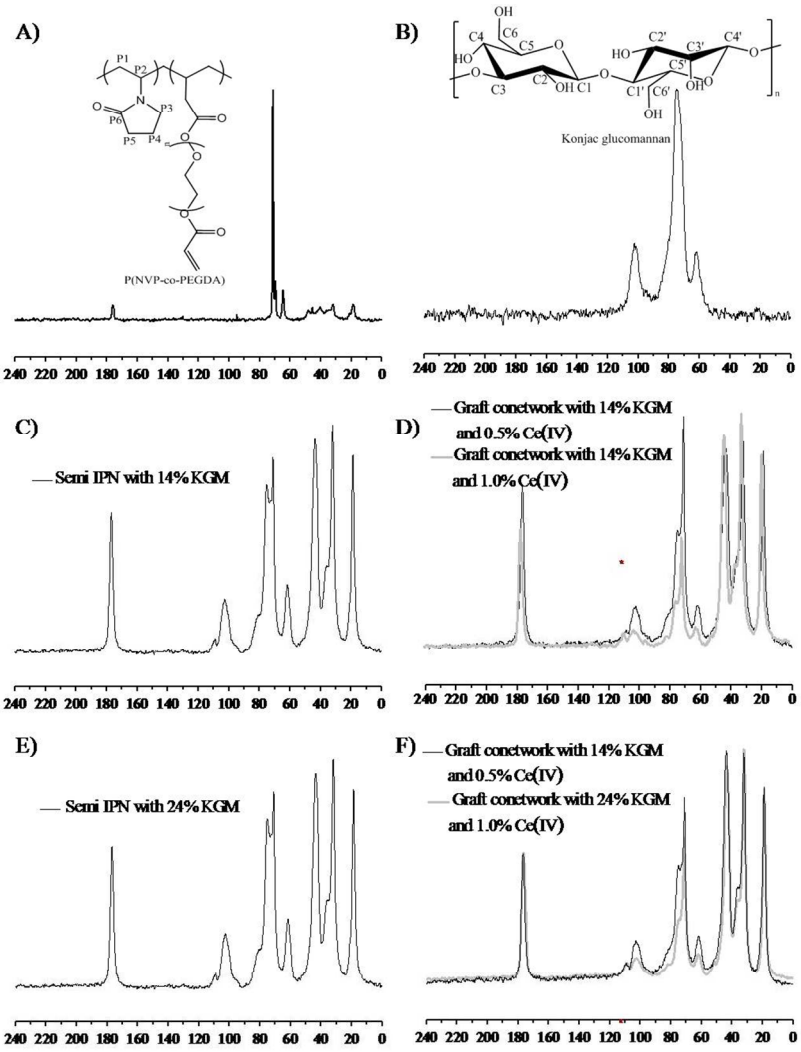

Figure 3. Solid state ^{13}C NMR spectra for A) P(NVP-co-PEGDA), B) crosslinked KGM with Ce(IV), C) semi-IPN 14 % KGM D) graft-conetwork 14% with 0.5% Ce(IV) (black) and 1% Ce(IV) (gray) , E) semi-IPN 24% KGM and F) graft-conetwork 24% with 0.5% Ce(IV) (black) and 1% Ce(IV) (gray).

High resolution solid state NMR spectroscopy (Figure 3) was used to characterize the solid polymers[30]. Useful assignments of the anomeric carbons C1, C3, C1'and C4' carbons had been already established previously for starch and cellulose[31] and in spectrum 3b these were observed as a broad but well-resolved peak around 105 ppm. Figure 3 shows ^{13}C Solid State NMR spectra for all of the hydrogels. In the spectrum 3A of P(NVP-co-PEGDA) the peak at 110 ppm, due to unreacted vinyl groups was absent[26]. However, a small peak in this region was observed in the semi-IPN and graft-conetwork hydrogels indicating that a portion of the PEGDA remained unreacted in the bicompoment networks. The anomeric resonances from the KGM around 105 ppm[32] were observed in all samples of semi-IPN and graft-conetwork hydrogels as was the resonance derived from the P6 carbonyl of NVP residues. Both peaks were well-resolved from the others and served as clear and diagnostic indications of the bicomponent nature of the materials. There were differences observed in the relative intensity of the peaks in the graft-conetwork that were dependant on the amount of Ce(IV) used, suggesting changes in the composition of the materials, with the addition of Ce(IV). In KGM the broad peak around 75 ppm is assigned to the methylene hydroxyl carbons at C2, C4, C2' and C3'. C6 and C6' methylene carbons gave rise to a peak that was

	[Ce]	%Mol. feed [KGM]/NVP]	%Network composition [KGM]/NVP]
Conetwork	1.0	29.1	50
Conetwork	0.5	29.1	50
Conetwork	1.0	19.3	69
Conetwork	0.5	19.3	62
Semi-IPN	0	29.1	74
Semi-IPN	0	19.3	55

Table 1 Molar compositions expressed as percent KGM relative to NVP in the monomer feeds and polymerised networks.

almost resolved around 60 ppm and this was easily deconvoluted from the peak around 75 ppm. This methylene carbon could then be compared with the methylene on the NVP residues at P5 (approx. 19 ppm) to provide a reasonable estimate of the compositions of the graft-conetworks and the semi-IPNs. Table 1 provides the data showing the relative fractions of NVP (or PNVP residues) and glucose/mannose units in the feed and the polymerised materials. Moderate conversions of NVP and PEGDA produced materials that contained a larger proportion of KGM than in the feed.

3.2 Morphology of KGM hydrogels.

Figure 4 shows SEM micrographs of P(NVP-co-PEGDA), and hydrogels of 1% KGM with $1x10^{-3}$ % (w/v) Ce(IV), semi-IPNs and graft-conetworks with different concentrations of KGM and Ce(IV). The samples were prepared in moulds with the polymerizing mixtures pressed against poly(ethylene terephthalate) sheet. This process produced samples with smooth surfaces. However, the morphologies of the cross sections showed differences between P(NVP-co-PEGDA) and KGM containing hydrogels. Both the semi-IPNs and the graft-conetwork systems produced porous materials that were typical of reaction induced phase separation.

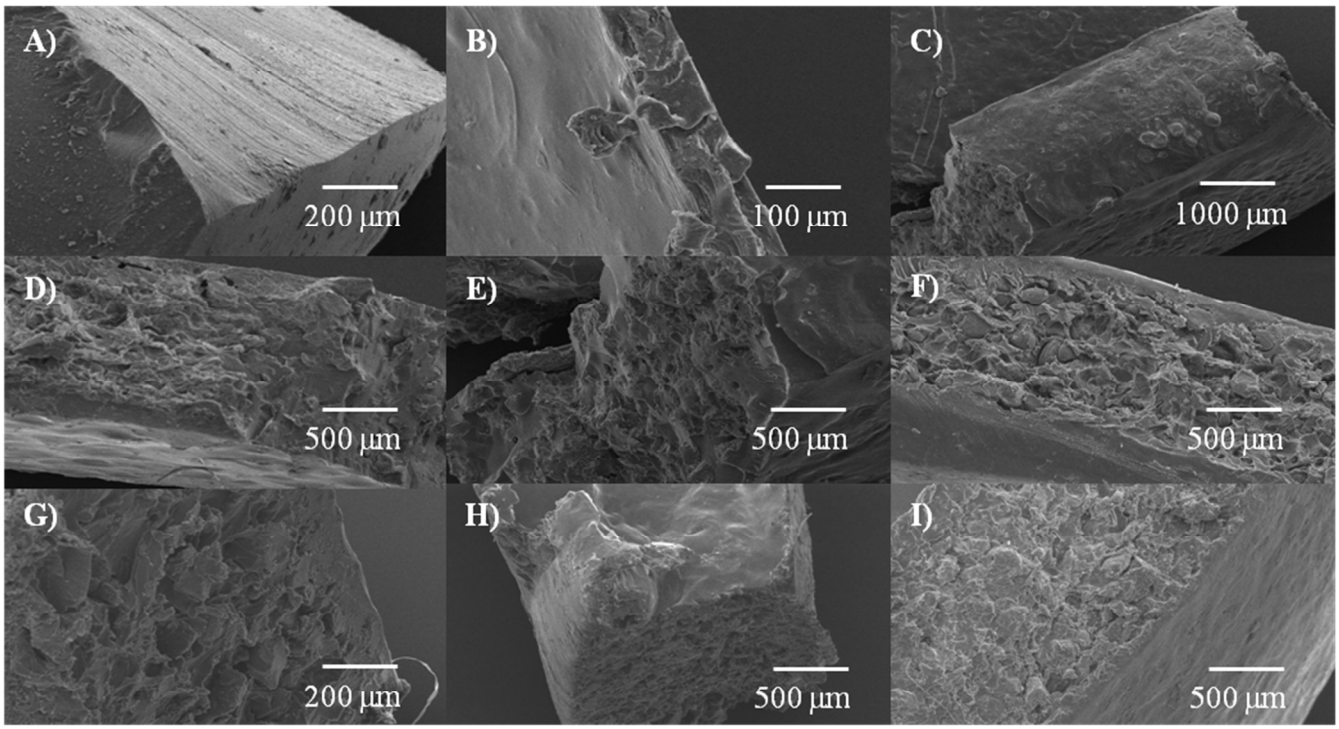

Figure 4. Scanning Electron Microscopy (SEM) micrographs of cross sections for A) P(NVP-co-PEGDA), B) crosslinked KGM with Ce(IV), (C-E) Semi-IPN of 14, 24 and 35% (w/v) KGM , (F-G) Graft-conetwork of 14% (w/v) KGM wt 0.5 and 1% (w/v) Ce(IV) respectively and (H-I) Graft-conetwork of 24% (w/v) KGM wt 0.5 and 1% (w/v) Ce(IV) respectively.

3.3 DSC analysis of dry networks

The thermal behaviours of crosslinked KGM, semi IPN and graft-conetworks were examined by DSC and the results are shown in Figure 5. The data from the crosslinked KGM material are provided in figure 5A. These data showed that KGM, without treatment with Ce(IV), provided a single endothermic peak stretching from 113 to 190°C, which we can assign to the glass transition temperature (T_g), with a peak maximum at 126°C. The addition of Ce(IV) was designed to introduce crosslinks by generating macroradicals on carbons next to the hydroxyls. In the absence of vinyl monomers or other compounds that could quench the radicals they can terminate bimolecularly producing crosslinks and this would be expected to increase the Tg. For most of the formulations a steady increase in the onset and peak temperatures was observed. However, $1x10^{-3}$ % (w/v) Ce(IV) gave a broader curve stretching between 80 and 190°C, with T_g at 118°C. The hydrogels with upto $1.5x10^{-3}$ % (w/v) Ce(IV) produced thermograms with one endothermic event but exothermic events were also observed in hydrogels with above this level of Ce(IV). These sharp exothermic peaks were at 185 and 217°C respectively and we suggest that they are due to degradation, which would be enhanced as the concentration of radicals increased: from increased [Ce(IV)]. Figure 5B shows the thermograms for semi-IPNs and grafted-conetworks of KGM and P(NVP-co-PEGDA) and shows an increase in the T_g with increasing concentrations of KGM and Ce(IV). P(NVP-co-PEGDA) showed a peak around 144°C and between 150 to 170°C. The complex nature of the thermal behaviour probably reflects the inhomogeneous nature of polymer networks prepared in this way. Heterogeneous compositions are common in similar polymerizations because polymer compositions change as conversion increases and in this type of polymerization this can

lead to changes in crosslink density. The semi-IPNs and graft conetworks appear to provide peaks that are combinations of the KGM and PNVP components but the exothermic events seen in Fig 5A were not observed.

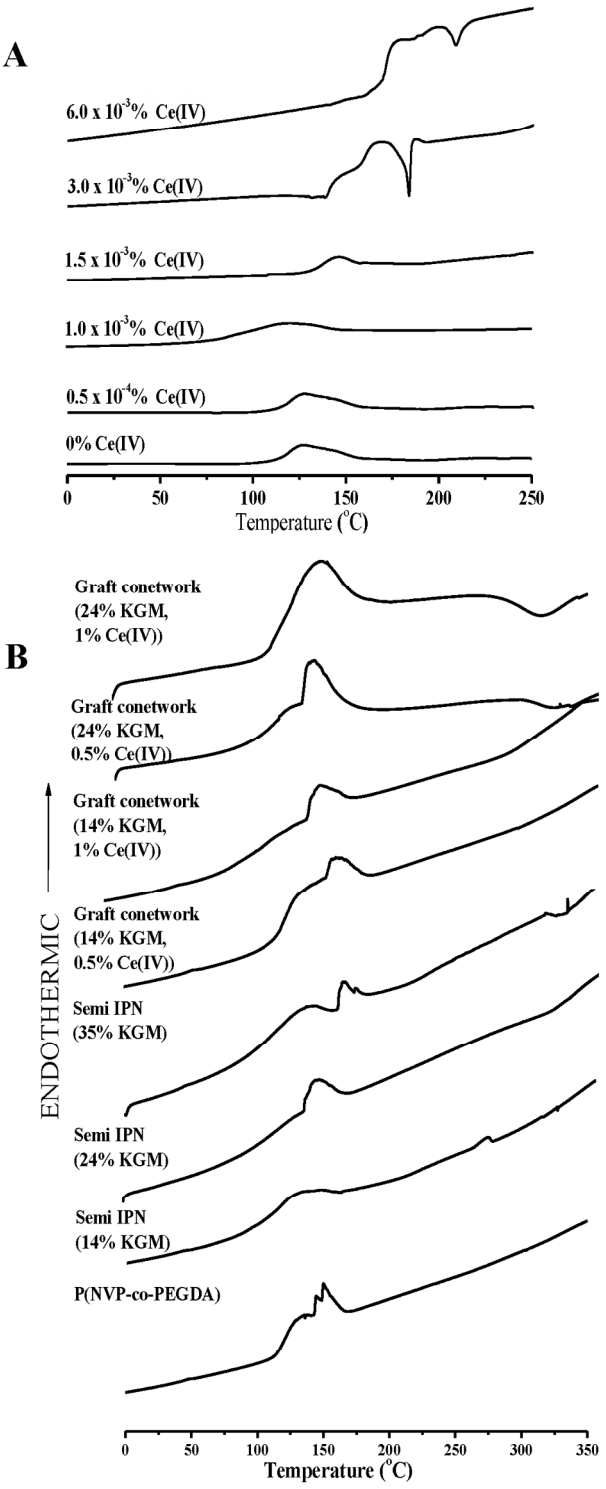

Figure 5. DSC thermograms derived from A) crosslinked KGM and B) non-swollen graft-conetworks and semi-IPNs

This appears to signify increased thermal stability in the multi-component materials, which could be rationalized by considering that polymerizations of NVP and PEGDA would compete with radical reactions on the KGM backbone. Although, crosslinking is mediated by the formation of macroradicals on the KGM backbone, high concentrations of radicals can also lead to side reactions such as elimination, which could lead to decreased thermal stability in the production of crosslinked KGM at high Ce(IV) concentration.

3.4 Analysis of water within the hydrogels

The swelling water within the hydrogels was examined using DSC by quantifying the amount of energy required to melt ice in the hydrogels when the samples were heated from -60 to 60°C at 1°C per min in hydrated conditions. Water-ice forms in hydrogels in phases where there are no, or only limited, interactions between the polymer and water. The exact nature of these freezing phases of water is often ill-defined and often more than one peak is observed in the DSC experiments. Another phase of the swelling water interacts, via hydrogen bonding with the polymer and these interactions prevent re-organization of the water molecules required for ice formation. Although, it is likely that the freezing water is composed of a continuum of interaction states, calorimetry can be used to assess the fractions of water represented by a generalized freezing state and the non-freezing/strongly interacting state. The structure of water in hydrogels appears to have an effect on a range of important properties including: diffusion of nutrients, cytokines and chemokines; cell adhesion and protein adsorption[40-42]. With these aspects in mind we considered that the architecture of the bicomponent hydrogels could affect the proportions of water in the different states as the polymer phase structure changes. These changes in both swelling and water structure could have an effect on biological properties. Figure 6A shows that the peak of the ice melting peaks occur between 5.2 to 6.4°C for the semi-IPNs and that this was substantially lower in the P(NVP-co-PEGDA) and graft-conetworks (1.8 to 2.7°C). The relationship between the energy required to melt the ice present per mass of water and the EWC is summarized in Figure 6B. At these high EWCs for materials containing KGM (semi-IPN and graft-conetwork) increased EWC appears to produce materials with larger fractions of the water in the freezable state. In general the graft-conetworks had lower EWCs than the semi-IPNs and as stated above this provided materials in which smaller fractions of the water could be frozen. Also, ice formed to a greater extent in the P(NVP-co-PEGDA) material than in any of the KGM-containing materials. This observation suggests that the interactions between water and the KGM are more extensive than the interactions of water with P(NVP-co-PEGDA).

3.5 The effects of KGM hydrogels on skin cells.

Cell metabolic activity was measured, with cells in indirect contact after 3 days using the MTT assay. The direct contact results (see ESI Table 2) show that neither increasing concentrations of Ce(IV), KGM, or the presence of P(NVP-co-PEGDA) affected cell metabolism. The effect of direct contact of KGM hydrogels with increasing concentrations of Ce(IV) and KGM on skin cells are shown in Figure 7(i). Keratinocyte metabolism was reduced after 3 and 5 days of direct contact with

hydrogels with increasing concentrations of Ce(IV) and KGM.

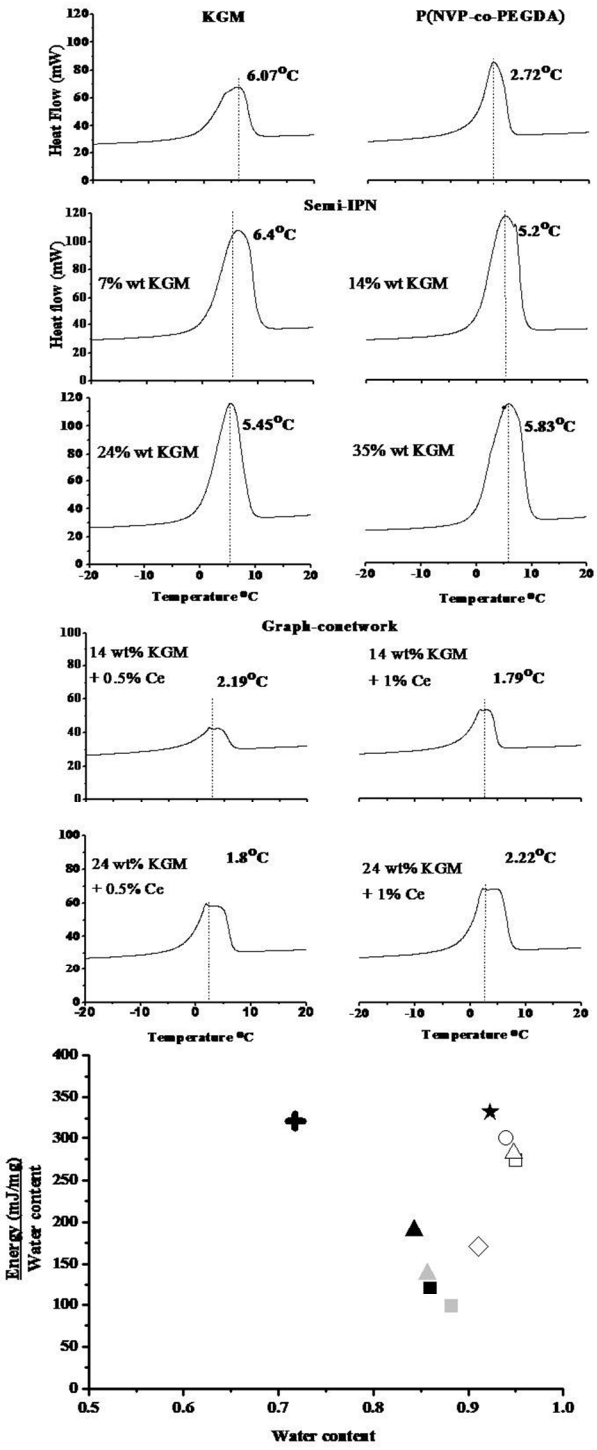

Figure 6 A) Water content of hydrogels. DSC thermograms of hydrated KGM, P(NVP-co-PEGDA), semi-IPN and graft-conetwork B) The relationship between free water total water content, measured by the amount of energy required to release the water from the hydrogel. ★ represents KGM in solution, P(NVP-co-PEGDA) +; semi-IPN with ○ 7% ; □ 14%; Δ 24% and ◊ 35% KGM. Graft-conetwork with 0.5% Ce(IV) (■ 14 % and ▲, 24%) and with 1.0% Ce(IV) ■ 14% and ▲ 24% KGM).

However, increasing concentrations of Ce(IV) inhibited fibroblast viability, while 0.5-1.25% (w/v) KGM stimulated fibroblast proliferation, and 1.5% (w/v) KGM did not (Figure 7(i) (B and D)). From these results, it appears that Ce(IV) inhibited both fibroblast and keratinocyte proliferation.

The direct contact of PNVP-containing hydrogels on fibroblasts measured after 3 and 5 days shows that graft-conetworks stimulated fibroblast viability, while semi-IPN and P(NVP-co-PEGDA) hydrogels did not (Section (ii), Figure 8 A-B). KGM containing semi-IPN and graft-conetwork hydrogels inhibited keratinocyte viability when placed adjacent with the cells after 48 hours (Figure 8).

3.6 The effect of semi and graft-conetwork on the migration of fibroblasts and keratinocytes in a wound scratch assay.

The effect of semi-IPN and graft-conetwork hydrogels on the migration of MMC mitomycin C treated fibroblasts and keratinocytes in a wound scratch assay were measured using image analysis after 24 and 48 hours, respectively. Figure 9 (A and B) shows the quantitative measurement of fibroblasts and keratinocyte migration. Scratches treated with graft-conetworks had closed completely by 36 hours, therefore a mid-point fix of 15 hours was chosen to look at differences between hydrogels. For keratinocytes, wounds treated with graft-conetwork closed completely by 48 hours and 24 hours was chosen to show differences between hydrogels. Graft-conetwork of 14% KGM with 1.0% Ce(IV) (w/v) and both 24% KGM with 0.5 and 1.0 % Ce(IV) (w/v) significantly stimulated the migration of both skin cells compared to the control, P(NVP-co-PEGDA), and semi IPNs.

The Live/Dead stained fibroblasts in a wound scratch assay after 36 hours (Figure 9C) shows the rapid migration of fibroblasts in the direct contact with graft-conetworks compared to semi IPNs and P(NVP-co-PEGDA). The micrographs also show the absence of dead cells, implying that all the hydrogels were cell-compatible.

4. Discussion

It was found that P(NVP-co-PEGDA), semi-IPN and graft-conetwork hydrogels were able to maintain their physical integrity in aqueous medium after 2-3 days compared to soluble and crosslinked KGM (see Table 2). The graft-conetwork and crosslinked KGM shared the same biological activities with native, soluble KGM in the stimulation and inhibition of fibroblast and keratinocyte viability. Whilst the semi-IPNs did not stimulate fibroblast proliferation, the direct contact of the hydrogels with keratinocytes inhibited their viability after 48 hours. We also confirmed that crosslinked KGM and graft-conetwork hydrogels were able to stimulate the migration of growth arrested fibroblasts and keratinocytes compared to soluble KGM and semi-IPN. From these results, we can see that all of the KGM containing hydrogels were biologically active compared to P(NVP-co-PEGDA).

In this study, crosslinked KGM and bicomponent (KGM and PNVP) hydrogels with semi-IPN and graft-conetwork architectures were synthesized and assessed in a range of cellular assays. A crosslinked KGM hydrogel was synthesized using oxidation of methylene adjacent to hydroxyl with Ce(IV) as a

source of main chain radicals.

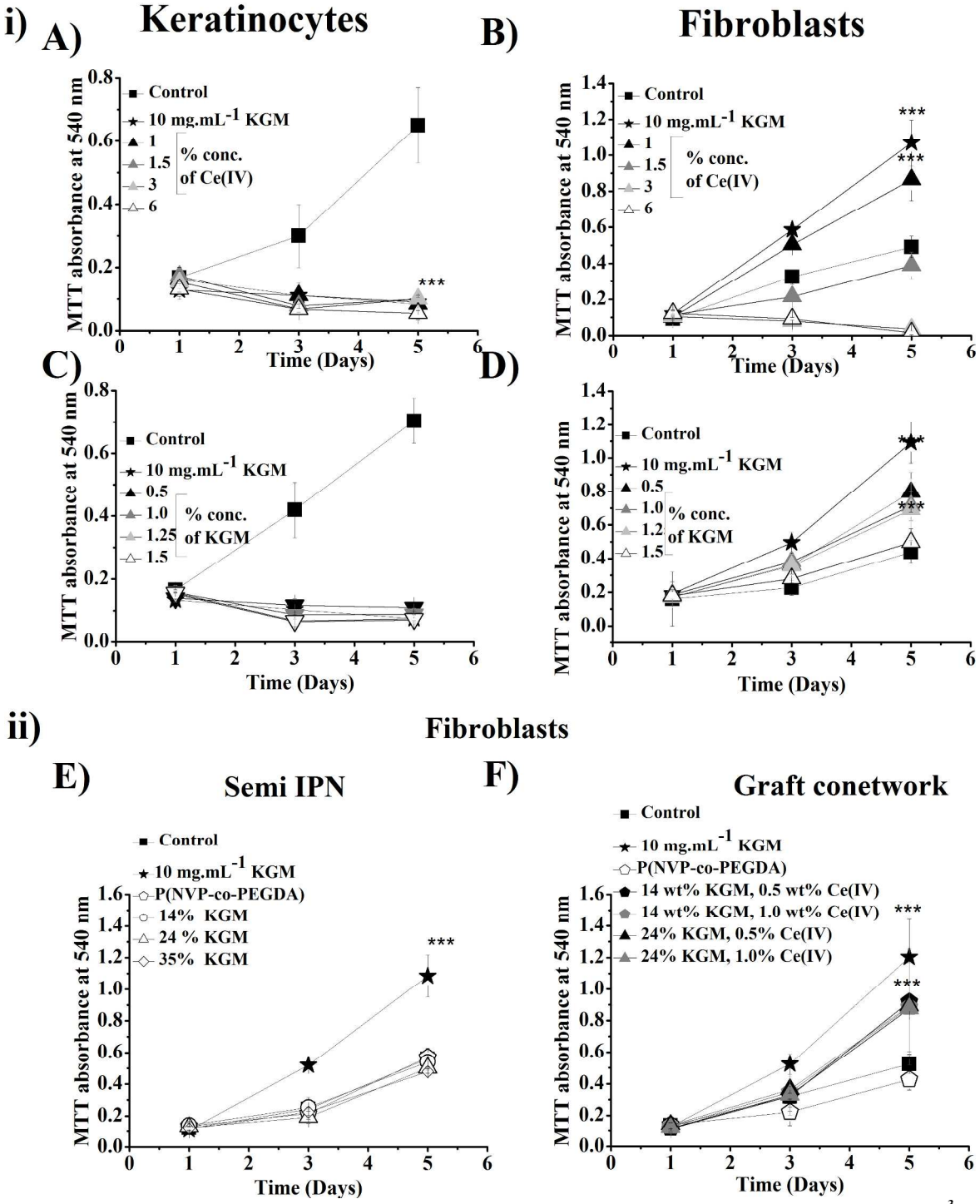

Figure 7 i) The effect of increasing concentrations of A-B) Ce(IV) with 1% KGM and C-D) KGM with $1x10^{-3}$% Ce(IV) in hydrogels in direct contact with keratinocytes and fibroblasts measured after 1, 3 and 5 days in culture using MTT assay. ii) The effect of (E) Semi IPN and (F) graft-conetwork hydrogels with different concentrations of KGM and Ce(IV) in direct contact with fibroblasts measured after 1, 3, and 5 days using MTT assay. 1 mL of $2x10^4$ fibroblasts were cultured in 10% DMEM or 1 mL of $2x10^4$ keratinocytes co-cultured with $2x10^4$ i3T3 in 10% Greens' in 12 well plate for overnight. Then, 0.79 cm^2 hydrogel was put in direct contact with the cells, respectively. Results shown are means ± SD, ***p<0.001 highly significant, **p<0.01 very significant and *p<0.05 significant compared to control. and n=3 (n: number of experiment with 3 replicates).

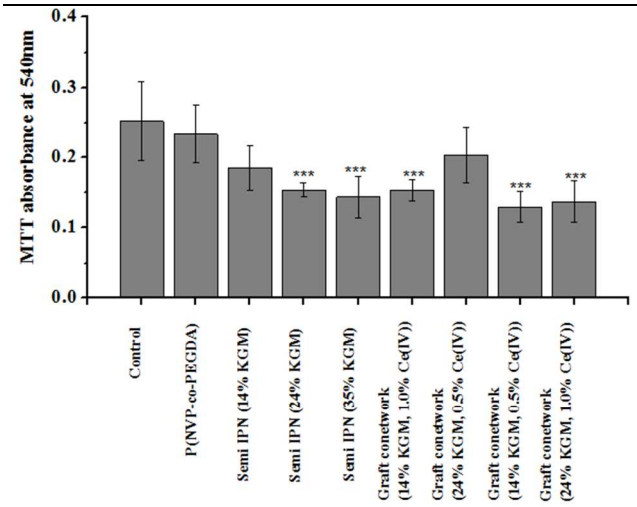

Figure 8. The effect of direct contact of semi and graft-conetwork on keratinocyte metabolic activity after 48 hours using MTT assay. $1x10^5$ keratinocytes co-cultured with $5x10^4$ i3T3 in 10% Green's in a 12 well plate overnight. Then, 0.79 cm^2 hydrogel was put in direct contact with the cells. Results shown are means ± SD, ***p<0.001 highly significant, **p<0.01 very significant and *p<0.05 significant compared to control and n=3 (n: number of experiment with 3 replicates).

Semi-IPNs and graft-conetworks were produced via photopolymerization of NVP and PEGDA using HMPP as an initiator. To produce graft conetworks Ce(IV) was used to initiate the grafting of P(NVP-co-PEGDA) to KGM as well as crosslinking the KGM by combination of KGM macroradicals prior to the photopolymerization.

PNVP and PEGDA are rigid polymers with T_gs at 158 and 54°C, respectively [33, 34] and a combination of both polymers gave a broad DSC thermograms with two shoulder peaks at 143 and 153°C, and a narrower peak at 143°C, indicating the presence of different chemical compositions within the samples. Endo and exothermic peaks were observed in the crosslinked KGM with $1.5x10^{-3}$ and $3x10^{-3}$ % Ce(IV), in semi-IPN with 35% KGM and graft-conetworks with 14% KGM and 0.5% Ce(IV). The endothermic peak was attributed to the T_g and increased with increasing concentrations of Ce(IV) as the crosslink density increased (indicated by reduced swelling). The exothermic peak, which can be associated with chain degradation, was observed as the concentration of Ce(IV) increased.

The presence of KGM in the hydrogels affected the internal morphology as shown in SEM micrographs. While the outer surfaces of all hydrogels showed smooth morphology, the cross section of KGM containing hydrogels had a porous structure.

Correlation between the changes in the chemical composition of KGM in semi-IPN and graft-conetwork and water interaction were investigated using EWC and calorimetry. The EWC of a hydrogel is of great interest for controlled release applications and hydrogel degradation. Hydrogels swell due to the osmotic potential of the hydrophilic chain, which drives water to diffuse into the network until the free energy is balanced by the increased elastic strain.

	KGM	KGM:Ce(IV)	P(NVP-co-PEGDA)	SemiIPN	Graft Conetwork
Stability (solubility)	Soluble	1-2 days	Non-degradable	Non-degradable	Non-degradable
Fibroblast metabolic activity (1-5 days)	↑↑↑	↑↑	No effect	No effect	↑↑
Keratinocyte metabolic activity (1-5 days)	↓↓↓	↓↓↓	No effect	↓↓↓	↓↓↓
Fibroblast migration (36 hours)	-	↑	No effect	No effect	↑
Keratinocyte migration (48 hours)	-	-	No effect	No effect	↑

Table 2. Summary of effects of hydrogels on skin cells. The effects of KGM hydrogels on keratinocytes and fibroblasts. Symbols represent (↑) increase, (↑↑) large increase, (↑↑↑) very large increase, (↓) decrease, (↓↓) large decrease, (↓↓↓) very large decrease, and (–) not done.

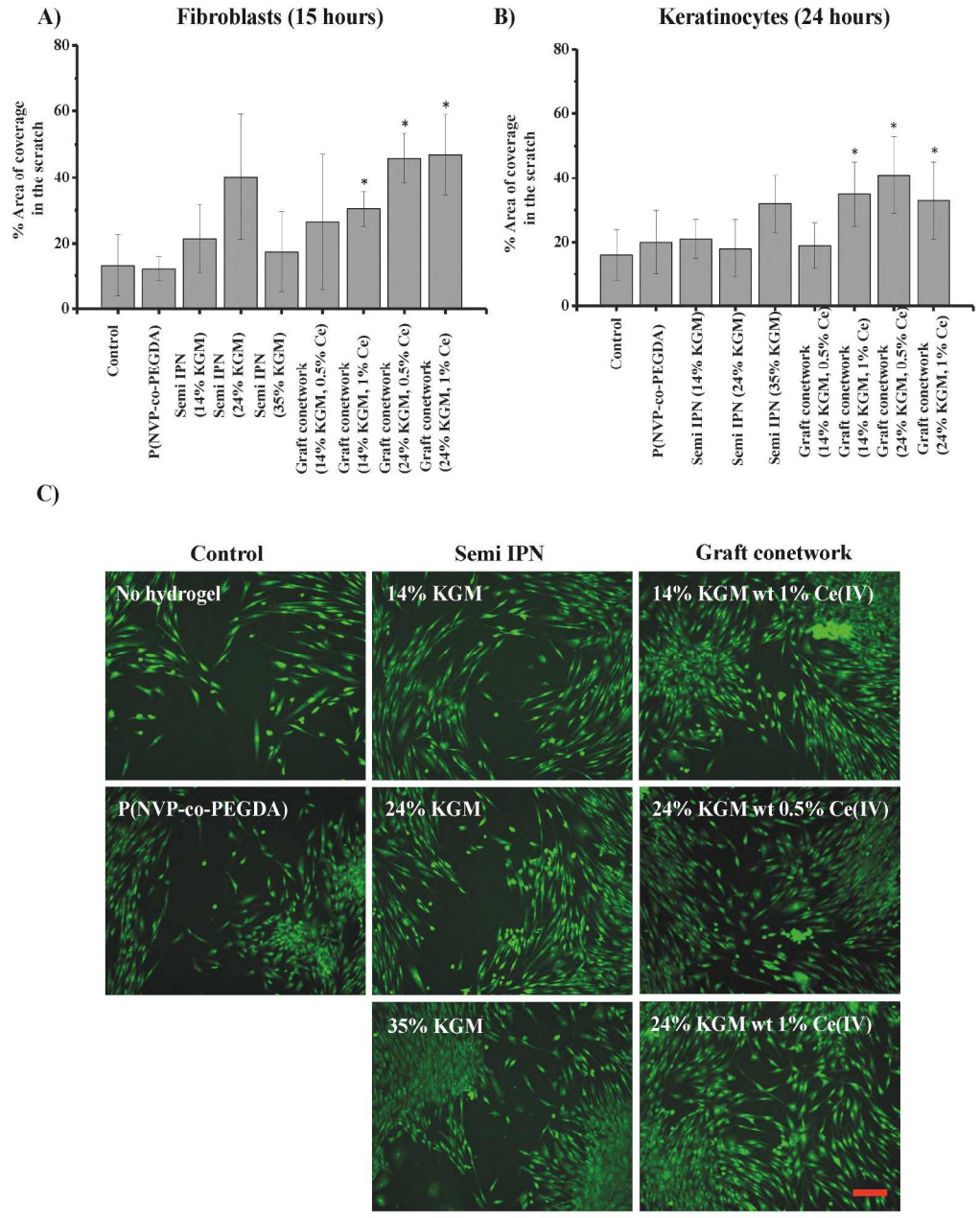

Figure 9. The effect of semi-IPN and graft-conetwork on the migration of A) fibroblasts and B) keratinocytes in a wound scratch assay. After 15 and 24 hours respectively, cells were photographed under phase contrast microscopy and the percentage of the filled area was compared to original scratch area (at 0 hour) and then calculated by image analysis using ImageJ. 1 mL of $2x10^4$ fibroblasts were cultured in 10% DMEM or $1x10^5$ keratinocytes co-cultured with $5x10^4$ i3T3 in 10% Green's in 12 well plate for overnight before being treated with 300 µL of 10 $\mu g.mL^{-1}$ MMC for 30 minutes or an hour, respectively. Then 0.79 cm^2 semi and graft-conetworks were put directly onto the cells. Results shown are means ± SD ***p<0.001 highly significant, **p<0.01 very significant and *p<0.05 significant compared to control and n=2, (n: number of experiment with 3 replicates). C) Microphotographs of Live/Dead stained fibroblasts with (Syto9 and PI) after 36 hours in direct contact with semi-IPN and graft-conetwork. Scale bar: 100 µm.

The EWC for semi-IPNs decreased from 95 to 86% with increasing concentrations of KGM (14, 24 and 35% (w/v)) whereas the EWC for graft-conetwork hydrogels were in the range of 82-85%. The porous structure and the formation of crosslinking in the semi-IPN and graft-conetwork had clear effects on the hydrogel's EWC and the structure of water (Figure 4 A and B). The decrease in freezing water in graft-conetworks compared to semi-IPN with the same concentration of KGM may relate to the changes in the chemistry of KGM when Ce(IV) was added into the formulation. There was a general trend observed from DSC measurements, that in KGM containing materials, as the EWC increased, the fraction of water that could freeze also increased.

It was also clear that the difference in the structure and chemical properties were parallel to changes in the activities of these gels on cells. The semi-IPNs had higher EWC, increased fractions of freezing water, and KGM content than graft-conetworks. Graft-conetworks were crosslinked by the addition of Ce(IV) leading to the decrease of EWC which although any causal relationship is difficult to establish, may be related to the difference in the performance between the semi-IPNs and the graft-conetworks. The results certainly suggest that the differences in the biological activities of the semi-IPN and graft-conetwork hydrogels are not controlled primarily by the chemical structure of the polymer (the chemical functionality of both systems is almost indistinguishable): rather the amount and structure of water in the hydrogel appears to be the significant distinguishing feature.

Also, the biological effects on the stimulation and inhibition of fibroblast and keratinocyte viability are the results of a dynamic interaction between the cells and the gels perhaps via cell specific receptors (i.e. lectin receptors)[38]. The effect also might be attributed to hydrogel's ability to absorb mitogens from the media and act as a reservoir to the cells [23], while at the same time acting as a buffer or sink for metabolic waste from the cells. The detailed mechanism of action clearly would require further studies, but given the graft-conetwork's ability to stimulate fibroblast viability, this class of material could be potentially useful for wound healing.

Although, the exact mechanism of this hydrogel's ability to stimulate fibroblast proliferation is not clear, we suggest that the differences in the concentrations of KGM and Ce(IV), EWC, and the balance of freezing and non-freezing water inside the semi-IPN and graft-conetwork are all factors that may be relevant to the effects on cell proliferation and migration. Similar results on the stimulation of fibroblast proliferation were observed in our previous study with P(NVP-co-DEGBAC) and P(NVP-co-EDGMA), where both the type of crosslinker and % EWC appear to affect the stimulation of fibroblast proliferation [23]. P(NVP-co-DEGBAC) with 85-92% EWC were more stimulatory to fibroblast proliferation than to P(NVP-co-EDGMA) with 95% or more EWC. These changes in water structure are often thought to play significant roles in the biological activity of hydrogels [35, 36] and we suggest that they can also have an effect on stimulation of cell proliferation. Regardless of the exact mechanism, the graft conetworks promote fibroblast migration and proliferation over keratinocyte migration and proliferation and, in this respect, these materials could provide a robust material that could form the basis of an active wound dressing that could promote wound healing.

5. Conclusion

The graft-conetwork composed of crosslinked KGM and P(NVP-co-PEGDA) is the most promising, of the classes of KGM-PNVP based materials studied here, for wound healing applications due to its ability to stimulate both fibroblast viability and migration compared to KGM, crosslinked KGM and semi-IPNs.

Acknowledgement

We would like to acknowledge Dr. David J. Apperley from EPSRC UK National Solid-state NMR Service, Durham for ^{13}C solid state NMR measurement.

Notes and references

[a] *Materials Science and Engineering Department, Kroto Research Institute, University of Sheffield, Broad Lane, S37HQ, Sheffield, United Kingdom Fax: +44 (0) 114 222 5995 Tel: +44 (0) 114 222 5945; E-mail: mtp09mss@shef.ac.uk, a.j.bullock@shef.ac.uk, s.macneil@shef.ac.uk.*
[b] *Department of Chemistry, University of Sheffield, S3 7HF Sheffield, United Kingdom Tel: +44(0) 144 9565; E-mail: s.rimmer@shef.ac.uk.*

† Electronic Supplementary Information (ESI) available: MTT data from indirect contact cell culture experiments showing no indirect toxicity from leacates. See DOI: 10.1039/b000000x/

1. L. Huang, R. Takahashi, S. Kobayashi, T. Kawase and K. Nishinari, *Biomacromolecules*, 2002, **3**, 1296-1303.
2. T. Kondo, T. Shinozaki, H. Oku, S. Takigami and K. Takagishi, *Journal of Tissue Engineering and Regenerative Medicine*, 2009, **3**, 361-367.
3. F. Alvarez-Mancenido, M. Landin, I. Lacik and R. Martinez-Pacheco, *International Journal of Pharmaceutics*, 2008, **349**, 11-18.
4. H. Zhang, C.-H. Gu, H. Wu, L. Fan, F. Li, F. Yang and Q. Yang, *BioFactors*, 2007, **30**, 227-240.
5. M. Shahbuddin, D. Shahbuddin, A. J. Bullock, H. Ibrahim, S. Rimmer and S. MacNeil, *Carbohydrate Research*, 2013.
6. M. Liu, J. Fan, K. Wang and Z. He, *Drug Delivery*, 2007, **14**, 397-402.
7. R. V. Shevchenko, S. L. James and S. E. James, *Journal of The Royal Society Interface*, 2010, **7**, 229-258.
8. G. D. Winter, *Nature*, 1962, **193**, 293-294.
9. C. Xiao, H. Liu, Y. Lu and L. Zhang, *Journal of Applied Polymer Science*, 2001, **81**, 1049-1055.
10. Y. Lu, L. Zhang and P. Xiao, *Polymer Degradation and Stability*, 2004, **86**, 51-57.
11. S. Farris, K. M. Schaich, L. Liu, L. Piergiovanni and K. L. Yam, *Trends in Food Science & Technology*, 2009, **20**, 316-332.
12. N. A. Peppas and A. G. Mikos, in *Hydrogels in Medicine and Pharmacy*, ed. N. A. Peppas, Boca Raton, 1986.
13. N. Peppas, Y. Huang, M. Torres-Lugo, J. Ward and J. Zhang, *Annu Rev Biomed Eng*, 2000, **2**, 9-29.
14. N. Peppas, K. Keys, M. Torres-Lugo and A. Lowman, *J Control Release*, 1999, **62**, 81-87.
15. G. Chaby, J-C. Guillaume, A. Dompmartin, J. L. Richard and A.Zagnoli, *Arch Dermatol*, 2007, **143**, 1297-1304.
16. L.-G. Chen, Z.-L. Liu and R.-X. Zhuo, *Polymer*, 2005, **46**, 6274-6281.
17. Q. Li, W. Qi, R. Su and Z. He, *J Biomater Sci Polym Ed*, 2009, **20**, 299-310.

18. N. A. Peppas, P. Bures, W. Leobandung and H. Ichikawa, *European Journal of Pharmaceutics and Biopharmaceutics*, 2000, **50**, 27-46.
19. S. Farris, K. M. Schaich, L. Liu, L. Piergiovanni and K. L. Yam, *Trends in Food Science & Technology*, 2009, **20**, 316-332.
20. A. S. Hoffman, *Advanced Drug Delivery Reviews*, 2002, **54**, 3-12.
21. M. T. Razzak, D. Darwis, Zainuddin and Sukirno, *Radiation Physics and Chemistry*, 2001, **62**, 107-113.
22. S. Rimmer, in *Synthesis of hydrogels for biomedical applications: control of structure and properties*, ed. S. Rimmer, Woodhead Publishing Limited, 2011, p. 269.
23. L. E. Smith, S. Rimmer and S. MacNeil, *Biomaterials*, 2006, **27**, 2806-2812.
24. M. Nik and M. Otto, *Journal of Immunological Methods*, 1990, **130**, 149-151.
25. S. B. Widjanarko, A. Nugroho and T. Estiasih, *African Journal of Food Science* 2011, **5**, 12-21.
26. Y. F. Hua, M. Zhang, C.-x. Fu, Z.-H. Chen and G. Chan, *Carbohydrate Res*, 2004, **339**, 2219-2224.
27. C. Xiao, S. Gao, H. Wang and L. Zhang, *Journal of Applied Polymer Science*, 2000, **76**, 509-515.
28. Q. Guo, J. Huang and X. Li, *European Polymer Journal*, 1996, **32**, 423-426.
29. K. Lewandowska, *Thermochimica Acta*, 2011, **517**, 90-97.
30. M. Kobayashi, I. Ando, T. Ishii and S. Amiya, *Macromolecules*, 1995, **28**, 6677-6679.
31. F. H. Larsen, M. Schöbitz and J. Schaller, *Carbohydrate Polymers*, 2012, **89**, 640-647.
32. S. E. C. Whitney, J. E. Brigham, A. H. Darke, J. S. G. Reid and M. J. Gidley, *Carbohydrate Research*, 1998, **307**, 299-309.
33. J. V. Cauich-Rodriguez, S. Deb and R. Smith, *Journal of Materials Science: Materials in Medicine*, 1996, **7**, 269-272.
34. A. Priola, G. Gozzelino, F. Ferrero and G. Malucelli, *Polymer*, 1993, **34**, 3653-3657.
35. M. S. Jhon and J. D. Andrade, *Journal of Biomedical Materials Research*, 1973, **7**, 509-522.
36. D. Pasqui, M. De Cagna and R. Barbucci, *Polymers*, 2012, **4**, 1517-1534.